ASME ©;
Proceedings of ASME Turbo Expo 2017: Turbomachinery Technical Conference and Exposition GT2017
June 26-30, 2017, Charlotte, NC, USA

GT2017-64023

FREQUENCY-DOMAIN SENSITIVITY ANALYSIS OF STABILITY OF NONLINEAR VIBRATIONS FOR HIGH-FIDELITY MODELS OF JOINTED STRUCTURES

E.P. Petrov

University of Sussex, School of Engineering and Informatics,
Brighton BN1 9QT, United Kingdom, Email: y.petrov@sussex.ac.uk

ABSTRACT

For the analysis of essentially nonlinear vibrations it is very important not only to determine whether the considered vibration regime is stable or unstable but also which design parameters need to be changed to make the desired stability regime and how sensitive is the stability of a chosen design of a gas-turbine structure to variation of the design parameters. In the proposed paper, an efficient method is proposed for a first time for sensitivity analysis of stability for nonlinear periodic forced response vibrations using large-scale models structures with friction, gaps and other types of nonlinear contact interfaces. The method allows using large-scale finite element models for structural components together with detailed description of nonlinear interactions at contact interfaces. The highly accurate reduced models are applied in the assessment of the sensitivity of stability of periodic regimes. The stability sensitivity analysis is performed in frequency domain with the multiharmonic representation of the nonlinear forced response amplitudes. Efficiency of the developed approach is demonstrated on a set of test cases including simple models and large-scale realistic blade model with different types of nonlinearities, including: friction, gaps, and cubic elastic nonlinearity.

INTRODUCTION

Gas-turbine engine structures are, as a rule, assembled jointed structures. The nonlinear interactions occur at the contact interfaces of these joints and they are caused by friction forces, gaps, variable contact areas, cubic nonlinearities due to Hertzian contacts, etc. Development of methods for analysis of nonlinear vibrations in gas turbine engines represents a major interest for the industry and attracts efforts of many researchers (e.g. see Refs. [1]-[8]). The efficient analysis of periodic vibration can be performed in frequency domain for realistic models of structures which customarily contain millions degrees of freedom (DOFs).

For the numerical analysis of the nonlinear dynamics it is very important to determine the stability property of the found nonlinear vibration regime: stable vibrations can exist in practice of engine operation and unstable vibrations are usually not practically achievable since a structure leaves these regimes even under very small perturbations which are inevitable in practical conditions.

The classical Floquet stability analysis (see Refs.[9], [10]) requires time integration of the equations for the perturbed motion and, therefore, exhibits insurmountable difficulties in the application to the large-scale finite element (FE) models of structures.

The analysis of the stability of nonlinear vibration regimes in frequency domain can significantly reduce the computation expense and some significant contributions have been done relatively recently for systems with rather restricted number of degrees of freedom (e.g. see Refs. [11]-[15]). In Ref.[16] an efficient frequency-domain method has been developed for analysis of stability of periodic regimes of nonlinear forced vibrations for realistic models of gas-turbine structures containing thousands and millions degrees of freedoms.

In the design process it is often not sufficient to obtain the stability characteristics of the nonlinear vibrations but it is important to know: (i) how the stability can be affected by inevitable small variations of the structure, contact interfaces or excitation levels and conditions and (ii) which design parameters can be changed to improve the stability and robustness of the structure operation. The sensitivity analysis of the stability of nonlinear vibrations to design parameters variation can provide very useful data to perform the design optimization and to assess

the stability of a structure under uncertainties and stochastic character of the design parameters and excitation conditions (e.g. see some of the possible use of the sensitivities in Ref. [17]). To the best of the author's knowledge there have not been methods till now which would allow stability sensitivity analysis of realistic industrial models of jointed structures.

In the proposed paper, this problem is addressed for a first time and an efficient method is developed for the multiharmonic analysis of the sensitivity for the stability of nonlinear steady-state vibrations of jointed structures using realistic FE models, which can contain millions DOFs.

First, frequency-domain stability equations are formulated in the form of quadratic eigenproblem and the stability factors are determined from the solution of this equation.

Then, the original method for analytical evaluation of the sensitivity of the stability factors to design parameter variation are derived. Two major types of the design parameters are considered here: (i) a case when the design parameters affect the FE model and dynamic properties of linear parts of the structures (such as geometry, material properties, natural frequencies, modal damping factors, etc.) and (ii) a case of contact interface parameters, e.g. friction coefficients, contact stiffness, clearance and interference values, etc. The auxiliary sensitivity problems are formulated and solved to support the stability sensitivity analysis: (i) the sensitivity of the natural frequencies of linear components of a structure – to calculate stability sensitivities with respect to linear model parameters and (ii) the sensitivity of the nonlinear forced response to contact interface parameters – to calculate stability sensitivities with respect to nonlinear contact interface parameters.

The method is developed for two variants of the structure modelling: (i) a variant when matrices of the full FE model of a structure are used in the stability analysis – such a model can be used only for small to moderate number of DOFs and (ii) a variant when the reduced stability equations are applied for the stability sensitivity analysis – which is applicable for high-fidelity FE modelling with very large number of DOFs.

The stability sensitivity are analysed for two major types of damping in linear components of a structure: (i) viscous damping and (ii) structural damping.

The method has been implemented in a computer code and the efficiency, accuracy and numerical properties of the method are demonstrated on a representative set of numerical examples, which include a simple 1 DOF nonlinear oscillator, a beam FE model and a turbine blade model comprising up to 160,000 DOFs with different types of nonlinearities.

FREQUENCY-DOMAIN NONLINEAR FORCED RESPONSE ANALYSIS

The equation of motion for the forced vibrations of a structure with nonlinear interactions at joints can be written in the form:

$$\boldsymbol{K}\boldsymbol{x} + \boldsymbol{C}\dot{\boldsymbol{x}} + \boldsymbol{M}\ddot{\boldsymbol{x}} + \boldsymbol{f}(\boldsymbol{x},\dot{\boldsymbol{x}},\ddot{\boldsymbol{x}}) = \boldsymbol{p}(t) \qquad (1)$$

where $\boldsymbol{x}(t)$ is a vector of displacements for all degrees of freedom in the structure considered; $\boldsymbol{K}$, $\boldsymbol{C}$ and $\boldsymbol{M}$ are structural stiffness, damping and mass matrices of finite element (FE) model of a structure and $\boldsymbol{p}(t)$ is a vector of excitation forces; $\boldsymbol{f}(\boldsymbol{x},\dot{\boldsymbol{x}},\ddot{\boldsymbol{x}})$ is a vector of nonlinear contact interface forces which, for a general case considered here, can be explicitly dependent on displacements, $\boldsymbol{x}$, velocities, $\dot{\boldsymbol{x}}$, and accelerations, $\ddot{\boldsymbol{x}}$, of the structural components. The contact forces occur in gas-turbine structures at the blade root joints of bladed discs, at contact surfaces of underplatform or tip dampers, at contact surfaces of adjacent interlock shrouds and at rubbing contacts between rotor and casing. The causes of nonlinear behaviour are usually friction forces, unilateral interaction at the pairing contact surfaces, gaps, varying contact stiffness properties, as in the case of Hertzian contacts, etc. A case of periodic excitation forces is considered: $\boldsymbol{p}(t) = \boldsymbol{p}\left(t + 2\pi/\omega\right)$, where ω is the principal excitation frequency and the steady-state periodic oscillations are studied.

The time variation of displacements, the nonlinear contact forces and the periodic excitation forces for the steady-state periodic regimes with known period $T = 2\pi/\omega$ are represented by a restricted Fourier series:

$$\boldsymbol{x}(t) = \boldsymbol{X}_0 + \sum_{j=1}^{n}\left(\boldsymbol{X}_j^{\mathrm{c}}\cos m_j\omega t + \boldsymbol{X}_j^{s}\sin m_j\omega t\right) == \boldsymbol{H}^T\boldsymbol{X} \qquad (2)$$

$$\boldsymbol{f}(\boldsymbol{x},\dot{\boldsymbol{x}},\ddot{\boldsymbol{x}}) = \boldsymbol{H}^T\boldsymbol{F}\ ; \quad \boldsymbol{p}(t) = \boldsymbol{H}^T\boldsymbol{P} \qquad (3)$$

where $\boldsymbol{H} = \left[\boldsymbol{I}, \boldsymbol{I}\cos\tilde{\omega}_1 t, \boldsymbol{I}\sin\tilde{\omega}_1 t, ..., \boldsymbol{I}\sin\tilde{\omega}_n t\right]^T$; $\boldsymbol{I}\left(N\times N\right)$ is the identity matrix and N is the total number of DOFs in the structure; $\boldsymbol{X} = \left\{\boldsymbol{X}_0, \boldsymbol{X}_1^c, ..., \boldsymbol{X}_n^s\right\}^T$, $\boldsymbol{F} = \left\{\boldsymbol{F}_0, \boldsymbol{F}_1^c, ..., \boldsymbol{F}_n^s\right\}^T$; $\boldsymbol{P} = \left\{\boldsymbol{P}_0, \boldsymbol{P}_1^c, ..., \boldsymbol{P}_n^s\right\}^T$ are vectors of harmonic coefficients for displacements, nonlinear forces and excitation forces respectively; $\tilde{\omega}_j = m_j\omega$ are frequencies of the harmonic components used in the multiharmonic representation of displacements. The usual harmonic balance procedure gives the following nonlinear equation with respect to vector, $\boldsymbol{X}$:

$$\left[\tilde{\boldsymbol{K}} + \tilde{\boldsymbol{C}}\boldsymbol{E}_1 - \tilde{\boldsymbol{M}}\boldsymbol{E}_2\right]\boldsymbol{X} + \boldsymbol{F}\left(\boldsymbol{X}\right) = \boldsymbol{P} \qquad (4)$$

where $\tilde{\boldsymbol{M}} = diag(\boldsymbol{M},...,\boldsymbol{M})$; $\tilde{\boldsymbol{C}} = diag(\boldsymbol{C},...,\boldsymbol{C})$; $\tilde{\boldsymbol{K}} = diag(\boldsymbol{K},...,\boldsymbol{K})$;

$$\boldsymbol{E}_1 = diag\left(\boldsymbol{0}, \tilde{\omega}_1\begin{bmatrix}\boldsymbol{0} & \boldsymbol{I}\\ -\boldsymbol{I} & \boldsymbol{0}\end{bmatrix}, ..., \tilde{\omega}_n\begin{bmatrix}\boldsymbol{0} & \boldsymbol{I}\\ -\boldsymbol{I} & \boldsymbol{0}\end{bmatrix}\right) \qquad (5)$$

$$\boldsymbol{E}_2 = diag\left(\boldsymbol{0}, \tilde{\omega}_1^2\boldsymbol{I}, \tilde{\omega}_1^2\boldsymbol{I}, \tilde{\omega}_2^2\boldsymbol{I}, \tilde{\omega}_2^2\boldsymbol{I}, ..., \tilde{\omega}_n^2\boldsymbol{I}\right) \qquad (6)$$

The nonlinear equation is solved by the Newton-Raphson iterations as described in Ref.[4]:

FREQUENCY-DOMAIN STABILITY EQUATIONS

In this section a brief review of the frequency-domain formulation is given as an introduction to the stability sensitivity analysis, more details can be found in Ref. [16].

Full model stability formulation

When the solution, $\boldsymbol{x}^*$, is found then we can represent the perturbed motion as $\boldsymbol{x} = \boldsymbol{x}^* + e^{\lambda t}\boldsymbol{s}$ and the time-domain stability

equation is obtained by linearization of Eq.(1):

$$\left[\boldsymbol{M}+\frac{\partial \boldsymbol{f}}{\partial \ddot{\boldsymbol{x}}}\right]\left(\lambda^2\boldsymbol{s}+2\lambda\dot{\boldsymbol{s}}+\ddot{\boldsymbol{s}}\right)+\left[\boldsymbol{C}+\frac{\partial \boldsymbol{f}}{\partial \dot{\boldsymbol{x}}}\right]\left(\lambda\boldsymbol{s}+\dot{\boldsymbol{s}}\right)+\left[\boldsymbol{K}+\frac{\partial \boldsymbol{f}}{\partial \boldsymbol{x}}\right]\boldsymbol{s}=\boldsymbol{0} \quad (7)$$

The eigenvector function, $\boldsymbol{s}$, is represented by the multiharmonic expansion:

$$\boldsymbol{s}(t)=\boldsymbol{S}_0+\sum_{j=1}^{n_S}\left(\boldsymbol{S}_j^{\mathrm{c}}\cos k_j\omega t+\boldsymbol{S}_j^{s}\sin k_j\omega t\right)=\boldsymbol{H}_S^T\boldsymbol{S} \quad (8)$$

where $\boldsymbol{S}=\left\{\boldsymbol{S}_0,\boldsymbol{S}_1^c,...,\boldsymbol{S}_{n_S}^s\right\}^T$ is the vector of harmonic coefficients of the expansion for $\boldsymbol{s}(t)$ and $\boldsymbol{H}_S$ is constructed similar to matrix $\boldsymbol{H}$ used in the nonlinear forced response analysis. The application of the harmonic balance procedure gives the frequency domain stability equation:

$$\left[\lambda^2\boldsymbol{B}_2+\lambda\boldsymbol{B}_1+\boldsymbol{B}_0\right]\boldsymbol{S}=\boldsymbol{0} \quad (9)$$

This is a quadratic eigenproblem equation with respect to $\boldsymbol{S}$ and λ and the matrices involved here have the form:

$$\boldsymbol{B}_0=\tilde{\boldsymbol{K}}+\tilde{\boldsymbol{C}}\boldsymbol{E}_1-\tilde{\boldsymbol{M}}\boldsymbol{E}_2+\hat{\boldsymbol{K}} \quad (10)$$

$$\boldsymbol{B}_1=2\tilde{\boldsymbol{M}}\boldsymbol{E}_1+2\hat{\boldsymbol{M}}_1+\tilde{\boldsymbol{C}}+\hat{\boldsymbol{C}}\;;\quad \boldsymbol{B}_2=\tilde{\boldsymbol{M}}+\hat{\boldsymbol{M}}_2 \quad (11)$$

The matrices corresponding to the nonlinear forces are indicated by a cap '∧' above the symbol and they are defined as:

$$\hat{\boldsymbol{K}}=\frac{\partial \boldsymbol{F}}{\partial \boldsymbol{X}}\;;\quad \hat{\boldsymbol{C}}=\frac{2}{T}\int_0^T\boldsymbol{H}_S^*\frac{\partial \boldsymbol{f}}{\partial \dot{\boldsymbol{x}}}\boldsymbol{H}_S^T dt \quad (12)$$

$$\hat{\boldsymbol{M}}_1=\frac{2}{T}\int_0^T\boldsymbol{H}_S^*\frac{\partial \boldsymbol{f}}{\partial \ddot{\boldsymbol{x}}}\dot{\boldsymbol{H}}_S^T dt\;;\quad \hat{\boldsymbol{M}}_2=\frac{2}{T}\int_0^T\boldsymbol{H}_S^*\frac{\partial \boldsymbol{f}}{\partial \ddot{\boldsymbol{x}}}\boldsymbol{H}_S^T dt \quad (13)$$

where matrix $\boldsymbol{H}_S^*$ used in the harmonic balance procedure differs from $\boldsymbol{H}_S$ only by a multiplier 0.5 for the components corresponding to zero harmonic (see Ref.[4]).

Reduced stability formulation

The large finite element models used by the gas-turbine industry can contain 10^5 – 10^6 DOFs. To estimate the solution stability all eigenvalues of Eq. (9) have to be calculated.

This problem is very time consuming and, hence, it is not practical to solve it directly for full finite element models due to very large computational time. In Ref. [16] a method for reduction of the model size has been proposed. The reduction is achieved by expression of the vector of harmonic coefficient for all DOFs of the model through a linear combination of mode shapes of a linear structure:

$$\boldsymbol{S}=\tilde{\boldsymbol{\Phi}}\boldsymbol{c} \quad (14)$$

where $\tilde{\boldsymbol{\Phi}}=diag\left(\boldsymbol{\Phi},\boldsymbol{\Phi},...\boldsymbol{\Phi}\right)$; $\boldsymbol{\Phi}(N\times m)$ is a matrix of mass-normalised mode shapes of a linear structure calculated for a structure with the absence of the contact interactions; m is the number of mode shapes used for the model reduction. In order to calculate $\boldsymbol{\Phi}$ the following auxiliary eigenproblem is solved

$$\boldsymbol{K}\boldsymbol{\Phi}=\boldsymbol{M}\boldsymbol{\Phi}\boldsymbol{\Omega}^2 \quad (15)$$

The solution of this eigenproblem provides a matrix of eigenvectors $\boldsymbol{\Phi}$ and a matrix of natural frequencies corresponding to the eigenvectors: $\boldsymbol{\Omega}=diag\left(\omega_1,\omega_2,...,\omega_m\right)$. Substituting Eq.(14) in Eq.(9) and then projecting this equation on the mode shapes, $\boldsymbol{\Phi}$, gives us the following reduced stability equations:

$$\left[\lambda^2\boldsymbol{B}_2^r+\lambda\boldsymbol{B}_1^r+\boldsymbol{B}_0^r\right]\boldsymbol{c}=\boldsymbol{0} \quad (16)$$

where the matrices are expressed in the form:

$$\boldsymbol{B}_0^r=\tilde{\boldsymbol{\Omega}}^2+\tilde{\boldsymbol{C}}^r\boldsymbol{E}_1^r-\boldsymbol{E}_2^r+\tilde{\boldsymbol{\Phi}}^T\hat{\boldsymbol{K}}\tilde{\boldsymbol{\Phi}} \quad (17)$$

$$\boldsymbol{B}_1^r=2\boldsymbol{E}_1^r+\tilde{\boldsymbol{C}}^r+2\tilde{\boldsymbol{\Phi}}^T\hat{\boldsymbol{M}}_1\tilde{\boldsymbol{\Phi}}+\tilde{\boldsymbol{\Phi}}^T\hat{\boldsymbol{C}}\tilde{\boldsymbol{\Phi}}\;;\quad \boldsymbol{B}_2^r=\tilde{\boldsymbol{I}}^r+\tilde{\boldsymbol{\Phi}}^T\hat{\boldsymbol{M}}_2\tilde{\boldsymbol{\Phi}} \quad (18)$$

$\tilde{\boldsymbol{\Omega}}=diag\left(\boldsymbol{\Omega},\boldsymbol{\Omega},,...,\boldsymbol{\Omega}\right)$; the expressions for matrices $\boldsymbol{E}_1^r$ and $\boldsymbol{E}_2^r$ are similar to those given in Eqs.(5) and (6), but of the reduced size and $\tilde{\boldsymbol{I}}^r$ is the identity matrix. Two types of linear damping can be modelled: (i) viscous damping and (ii) frequency-independent, structural damping. For the viscous damping, the expression for the reduced linear damping matrix takes the form:

$$\tilde{\boldsymbol{C}}^r=diag(\boldsymbol{\Xi\Omega},\boldsymbol{\Xi\Omega},...\boldsymbol{\Xi\Omega})=\tilde{\boldsymbol{\Xi}}\tilde{\boldsymbol{\Omega}} \quad (19)$$

where $\tilde{\boldsymbol{\Xi}}=diag(\boldsymbol{\Xi},\boldsymbol{\Xi},...\boldsymbol{\Xi})$; $\boldsymbol{\Xi}=diag\left(\eta_1,\eta_2,...,\eta_m\right)$ and η_j are prescribed values of modal damping. For the structural damping the reduced frequency-independent damping matrix expressed in the form:

$$\tilde{\boldsymbol{C}}^r=\omega^{-1}diag(\boldsymbol{\Xi\Omega}^2,\boldsymbol{\Xi\Omega}^2,...\boldsymbol{\Xi\Omega}^2)=\omega^{-1}\tilde{\boldsymbol{\Xi}}\tilde{\boldsymbol{\Omega}}^2 \quad (20)$$

STABILITY SENSITIVITY CALCULATION

To assess the stability, all eigenvalues, λ_j, are calculated. Since the matrices of the considered eigenproblems comprise only real numbers, the eigenvalues and corresponding eigenvectors can be: (i) real numbers and (ii) complex numbers. For the latter case, the eigenvalues form pairs since each complex eigenvalue and vector has its complex-conjugate counterpart. The real parts of eigenvalues λ_j define the growth or decay of a perturbation motion and the imaginary part characterises the frequency of the perturbed motion. If any one of the eigenvalues has a positive real part, then the found periodic motion is unstable. For the analysis of stability sensitivity to variation of parameters of in majority of cases only one eigenvalue with the largest real part need to be assessed.

Stability sensitivity equation

The matrices involved in the stability equations are generally not symmetric and their right and left eigenvectors differ. In order to calculate the stability sensitivity we need to determine these both eigenvector types, so the eigenproblem is formulated with respect to left and right eigenvectors in the form:

$$\boldsymbol{S}_l^H\left[\lambda^2\boldsymbol{B}_2+\lambda\boldsymbol{B}_1+\boldsymbol{B}_0\right]=\boldsymbol{0} \quad (21)$$

$$\left[\lambda^2\boldsymbol{B}_2+\lambda\boldsymbol{B}_1+\boldsymbol{B}_0\right]\boldsymbol{S}_r=\boldsymbol{0} \quad (22)$$

where subscripts '*l*' and '*r*' indicate left and right eigenvectors and superscript '*H*' indicates the Hermitian conjugate. The

solution of this eigenproblem can be made using readily available mathematical procedures for linear eigenproblems. To do this the quadratic eigenproblems of Eqs.(21) and (22) can be transformed, for example, to the following linear eigenproblems:

$$\begin{bmatrix} \boldsymbol{0} & \boldsymbol{I} \\ \boldsymbol{B}_0^T & \boldsymbol{B}_1^T \end{bmatrix} \begin{Bmatrix} \boldsymbol{S}_l \\ \lambda \boldsymbol{S}_l \end{Bmatrix} = \lambda \begin{bmatrix} \boldsymbol{I} & \boldsymbol{0} \\ \boldsymbol{0} & -\boldsymbol{B}_2^T \end{bmatrix} \begin{Bmatrix} \boldsymbol{S}_l \\ \lambda \boldsymbol{S}_l \end{Bmatrix} \quad (23)$$

$$\begin{bmatrix} \boldsymbol{0} & \boldsymbol{I} \\ \boldsymbol{B}_0 & \boldsymbol{B}_1 \end{bmatrix} \begin{Bmatrix} \boldsymbol{S}_r \\ \lambda \boldsymbol{S}_r \end{Bmatrix} = \lambda \begin{bmatrix} \boldsymbol{I} & \boldsymbol{0} \\ \boldsymbol{0} & -\boldsymbol{B}_2 \end{bmatrix} \begin{Bmatrix} \boldsymbol{S}_r \\ \lambda \boldsymbol{S}_r \end{Bmatrix} \quad (24)$$

Now, differentiating Eq.(22) with respect to the parameter for which we want to determine the stability sensitivity and then multiplying from the left by $\boldsymbol{S}_l^H$ we obtain the expression for the stability factor sensitivity:

$$\lambda' = -\boldsymbol{S}_l^H \left[\lambda^2 \boldsymbol{B}_2' + \lambda \boldsymbol{B}_1' + \boldsymbol{B}_0' \right] \boldsymbol{S}_r \Big/ w \quad (25)$$

where $w = \boldsymbol{S}_l^H \left[2\lambda \boldsymbol{B}_2 + \boldsymbol{B}_1 \right] \boldsymbol{S}_r$ and the prime indicates a full derivative with respect to a design parameter. Here the expressions are shown for a case of full matrix formulation, for the case of using the reduced stability equation they are obtained analogously.

Stability sensitivity with respect to parameters of a linear model

For the case when the stability sensitivity is required to be obtained with respect to variation of some design parameter of a linear part of the structure, e.g. to the variation of geometry, material characteristics, natural frequencies or modal damping the following calculation can be performed.

(i) For a case of full model formulation the stability sensitivity is obtained from:

$$\lambda' = -\boldsymbol{S}_l^H \left[\lambda^2 \tilde{\boldsymbol{M}}' + \lambda \left(2\tilde{\boldsymbol{M}}' \boldsymbol{E}_1 + \tilde{\boldsymbol{C}}' \right) + \tilde{\boldsymbol{K}}' + \tilde{\boldsymbol{C}}' \boldsymbol{E}_1 - \tilde{\boldsymbol{M}}' \boldsymbol{E}_2 \right] \boldsymbol{S}_r \Big/ w \quad (26)$$

where the derivatives of the structure mass, stiffness and damping matrices should be calculated with the respect to the parameter of interest.

(ii) For a case of the reduced stability formulation, the stability sensitivity is obtained from the following equation:

$$\lambda' = -\boldsymbol{c}_l^H \left[\tilde{\boldsymbol{C}}^{r\prime} \left(\lambda \boldsymbol{I} + \boldsymbol{E}_1^r \right) + 2\tilde{\boldsymbol{\Omega}} \tilde{\boldsymbol{\Omega}}' \right] \boldsymbol{c}_r \Big/ w \quad (27)$$

Therefore, for the case of viscous damping model we have:

$$\lambda' = -\boldsymbol{c}_l^H \left[\left(\tilde{\boldsymbol{\Xi}}' \tilde{\boldsymbol{\Omega}} + \tilde{\boldsymbol{\Xi}} \tilde{\boldsymbol{\Omega}}' \right) \left(\lambda \boldsymbol{I} + \boldsymbol{E}_1^r \right) + 2\tilde{\boldsymbol{\Omega}} \tilde{\boldsymbol{\Omega}}' \right] \boldsymbol{c}_r \Big/ w \quad (28)$$

and for structural damping the stability sensitivity takes the form:

$$\lambda' = -\boldsymbol{c}_l^H \left[\left(\tilde{\boldsymbol{\Xi}}' \tilde{\boldsymbol{\Omega}}^2 + 2\tilde{\boldsymbol{\Xi}} \tilde{\boldsymbol{\Omega}} \tilde{\boldsymbol{\Omega}}' \right) \left(\lambda \boldsymbol{I} + \boldsymbol{E}_1^r \right) + 2\tilde{\boldsymbol{\Omega}} \tilde{\boldsymbol{\Omega}}' \right] \boldsymbol{c}_r \Big/ (\omega w) \quad (29)$$

For the reduced stability formulation there is a possibility of the straightforward calculation of the stability factors with the respect to the variation of the modal properties of the structure: modal damping factors, η_j, and natural frequencies, ω_j, i.e.

- for viscous damping

$$\frac{\partial \lambda}{\partial \eta_j} = -\boldsymbol{c}_l^H \tilde{\boldsymbol{\Omega}}_j \left(\lambda \boldsymbol{I} + \boldsymbol{E}_1^r \right) \boldsymbol{c}_r \Big/ w \quad (30)$$

$$\frac{\partial \lambda}{\partial \omega_j} = -\boldsymbol{c}_l^H \left[\tilde{\boldsymbol{\Xi}}_j \left(\lambda \boldsymbol{I} + \boldsymbol{E}_1^r \right) + 2\tilde{\boldsymbol{\Omega}}_j \right] \boldsymbol{c}_r \Big/ w \quad (31)$$

- for structural damping

$$\frac{\partial \lambda}{\partial \eta_j} = -\boldsymbol{c}_l^H \tilde{\boldsymbol{\Omega}}_j^2 \left(\lambda \boldsymbol{I} + \boldsymbol{E}_1^r \right) \boldsymbol{c}_r \Big/ (\omega w) \quad (32)$$

$$\frac{\partial \lambda}{\partial \omega_j} = -\boldsymbol{c}_l^H \left[2\tilde{\boldsymbol{\Xi}} \tilde{\boldsymbol{\Omega}}_j \left(\lambda \boldsymbol{I} + \boldsymbol{E}_1^r \right) + 2\tilde{\boldsymbol{\Omega}}_j \right] \boldsymbol{c}_r \Big/ (\omega w) \quad (33)$$

where $\tilde{\boldsymbol{\Omega}}_j = diag\left(\boldsymbol{\Omega} \boldsymbol{e}_j, ..., \boldsymbol{\Omega} \boldsymbol{e}_j \right)$; $\tilde{\boldsymbol{\Xi}}_j = diag\left(\boldsymbol{\Xi} \boldsymbol{e}_j, ..., \boldsymbol{\Xi} \boldsymbol{e}_j \right)$ and $\boldsymbol{e}_j$ is a diagonal matrix with j-th diagonal element equal to 1 while all the other are zeros.

When the sensitivity is required with respect to the design parameters of the structure (e.g. characteristics of geometry or material), the sensitivities of the natural frequencies of the structure with respect to these parameters are determined by differentiating the eigenproblem equation for the linear structure given by Eq.(15):

$$\omega_j' = \phi_j^T \left(\boldsymbol{K}' - \omega_j^2 \boldsymbol{M}' \right) \phi_j \Big/ \left(2\omega_j \right) \quad (34)$$

The matrix $\tilde{\boldsymbol{\Omega}}'$ is then formed from these sensitivities. Moreover, applying the customarily acceptable assumption on the proportionality of the damping to the deformation energy, we can write the damping matrix sensitivity for both damping models:

viscous damping: $\boldsymbol{C}^{r\prime} = \eta \tilde{\boldsymbol{\Omega}}'$; structural damping: $\boldsymbol{C}^{r\prime} = 2\eta \tilde{\boldsymbol{\Omega}} \tilde{\boldsymbol{\Omega}}'$ (35)

These matrices, $\tilde{\boldsymbol{\Omega}}'$ and $\boldsymbol{C}^{r\prime}$, are then substituted in Eq.(27) to calculate the stability sensitivity factors.

Stability sensitivity with respect to parameters of nonlinear contact interfaces

The stability sensitivity can be also calculated with respect to parameters of nonlinear contact interfaces. Most common nonlinear interfaces which are considered in the analysis of assembled gas-turbine structures are gaps, cubic nonlinearity, friction contact interfaces. The parameters of these contact interfaces can be friction coefficient value, clearance or initial interference, contact stiffness, normal pressure, cubic nonlinearity stiffness coefficient and others.

For a case of full model formulation the stability sensitivity can be written in a general form:

$$\lambda' = -\boldsymbol{S}_l^H \left[\lambda^2 \hat{\boldsymbol{M}}_2' + \lambda \left(2\hat{\boldsymbol{M}}_1' + \hat{\boldsymbol{C}}' \right) + \hat{\boldsymbol{K}}' \right] \boldsymbol{S}_r \Big/ w \quad (36)$$

For a case of the reduced stability equation this expression takes the form:

$$\lambda' = -\boldsymbol{S}_l^H \tilde{\boldsymbol{\Phi}}^T \left[\lambda^2 \hat{\boldsymbol{M}}_2' + \lambda \left(2\hat{\boldsymbol{M}}_1' + \hat{\boldsymbol{C}}' \right) + \hat{\boldsymbol{K}}' \right] \tilde{\boldsymbol{\Phi}} \boldsymbol{S}_r \Big/ w \quad (37)$$

For a rather common case, when the nonlinear forces are dependent only on displacements and velocities, i.e. when the accelerations are not included explicitly in the nonlinear force formulation, the expressions for the stability factor sensitivity to the parameter of nonlinear contact interfaces are simplified:

for full formulation for reduced formulation

$$\lambda' = -\boldsymbol{S}_l^H \hat{\boldsymbol{K}}' \boldsymbol{S}_r / w; \qquad \lambda' = -\boldsymbol{S}_l^H \tilde{\boldsymbol{\Phi}}^T \hat{\boldsymbol{K}}' \tilde{\boldsymbol{\Phi}} \boldsymbol{S}_r / w \qquad (38)$$

In contrast to the sensitivity calculation with respect to linear model parameters the matrices involved in stability sensitivity to nonlinear contact interfaces are dependent not only on the interface parameters but also on the deformation of the structure, hence, the sensitivity of the tangent stiffness matrix of the contact interface interactions have to be determined in the form:

$$\hat{\boldsymbol{K}}' = \frac{d\hat{\boldsymbol{K}}(\boldsymbol{X}, p)}{dp} = \frac{\partial \hat{\boldsymbol{K}}}{\partial \boldsymbol{X}} \frac{\partial \boldsymbol{X}^*}{\partial p} + \frac{\partial \hat{\boldsymbol{K}}}{\partial p} = \frac{\partial}{\partial \boldsymbol{X}} \left(\hat{\boldsymbol{K}} \frac{\partial \boldsymbol{X}^*}{\partial p} \right) + \frac{\partial \hat{\boldsymbol{K}}}{\partial p} \qquad (39)$$

where p is the parameter for which the stability sensitivity is calculated and $\partial \boldsymbol{X}^* / \partial p$ is the sensitivity of the solution of the nonlinear forced response to this parameter. The sensitivities of the other matrices, $\hat{\boldsymbol{C}}'$, $\hat{\boldsymbol{M}}_1'$ and $\hat{\boldsymbol{M}}_2'$ describing the nonlinear interaction are expressed analogously.

All these expressions for the nonlinear stiffness, damping and mass matrix sensitivities involve the expressions, $\partial \boldsymbol{X}^* / \partial p$, for the sensitivity of the solution of the multiharmonic equation of motion, Eq.(4). These sensitivities are calculated from the equation obtained by the differentiation of Eq.(4) with respect to the design parameter of interest, p:

$$\left[\tilde{\boldsymbol{K}} + \hat{\boldsymbol{K}} + \tilde{\boldsymbol{C}} \boldsymbol{E}_1 - \tilde{\boldsymbol{M}} \boldsymbol{E}_2 \right] \frac{\partial \boldsymbol{X}^*}{\partial p} = -\frac{\partial \boldsymbol{F}}{\partial p} \qquad (40)$$

The nonlinear stiffness matrix, $\hat{\boldsymbol{K}}$, and vector of the sensitivity of nonlinear forces, $\partial \boldsymbol{F} / \partial p$ are evaluated here for the solution X^* taken from the last iteration of the Newton-Raphson solution process. The obtained vector, $\partial \boldsymbol{X}^* / \partial p$ is then substituted in Eq.(39) (and analogous expressions written for $\hat{\boldsymbol{C}}'$, $\hat{\boldsymbol{M}}_1'$ and $\hat{\boldsymbol{M}}_2'$) where it is treated as a constant vector when the derivative for the product of the stiffness matrix and vector $\partial \boldsymbol{X}^* / \partial p$ is calculated. One can see, that the calculation of stability sensitivity requires evaluation several additional vectors and matrices, which describe the contact interface behaviour, are needed for the analysis of the stability sensitivity. These are:

- the sensitivity of nonlinear contact force vector with respect to parameter variation: $\partial \boldsymbol{F} / \partial p$
- the sensitivity of the nonlinear stiffness matrix with respect to parameter variation: $\partial \hat{\boldsymbol{K}} / \partial p$;
- the sensitivity of the product of the stiffness matrix and the vector of solution sensitivity with respect to solution variations: $\partial \left(\hat{\boldsymbol{K}} \, \partial \boldsymbol{X}^* / \partial p \right) / \partial \boldsymbol{X}$.

If the nonlinear forces are explicitly dependent on the velocities then also matrices: $\partial \hat{\boldsymbol{C}} / \partial p$ and $\partial \left(\hat{\boldsymbol{C}} \, \partial \boldsymbol{X}^* / \partial p \right) / \partial \boldsymbol{X}$ and, in rare cases when these forces are functions of accelerations, then matrices $\partial \hat{\boldsymbol{M}}_1 / \partial p$, $\partial \hat{\boldsymbol{M}}_2 / \partial p$, $\partial \left(\hat{\boldsymbol{M}}_1 \, \partial \boldsymbol{X}^* / \partial p \right) / \partial \boldsymbol{X}$ and $\partial \left(\hat{\boldsymbol{M}}_2 \, \partial \boldsymbol{X}^* / \partial p \right) / \partial \boldsymbol{X}$ have to be calculated too.

The expressions of these additional matrices have been derived for node-to-node multiharmonic contact interactions analytically. The major types of nonlinear contact interactions have been considered: friction contact with gaps and variable normal load; gaps, cubic nonlinearity and some others. Some details of the analytical evaluation of these matrices can be found in Refs.[19] and [20].

NUMERICAL EXAMPLES

The methodology of stability sensitivity analysis has been introduced in a computer code. Some examples of stability sensitivity analysis for a simple model and for complex structures are given below. The simple models are used mostly for the method validation and exploration of sensitivity properties for typical nonlinearities and the complex models illustrate the capabilities of the method for analysis of realistic structures.

A simple model with different nonlinearity types

First example is a one-degree of freedom model described by the following equation:

$$m\ddot{x} + c\dot{x} + kx + f(x) = p \sin \omega t \qquad (41)$$

where $k = 40$; $m = 1$; $c = 0.1/\sqrt{40}$; $p = 100$ and $f(x)$ is the nonlinear force and the cases of nonlinear interaction caused by the following types of the nonlinear interactions are considered here: (i) a cubic nonlinear spring, (ii) a gap nonlinearity and (iii) friction contact.

For the analysis of nonlinear vibration the frequency range from 5 to 30 rad/s has been analysed and in the multiharmonic balance method all harmonics from 0 to 10 are included in the analysis. The number of non-zero harmonics kept in the stability equations is varied for some cases from 1 to 10. Since the system considered has one DOF there are two stability factors defining the periodic vibration regime stability. These two stability factors are selected from the total number of 42 eigenvalues obtained from the solution of the multiharmonic quadratic stability eigenproblem. The sensitivity is calculated for these two stability factors simultaneously with the nonlinear forced response analysis and the stability analysis.

In order to understand the formation of the stability factors for this oscillator, before the analysis of effects of nonlinearities on the forced response stability and its sensitivity, such analysis has been performed for a linear model, i.e. assuming that $f(x) \equiv 0$. The amplitude and real and imaginary parts of the stability factors are plotted as a function of the excitation frequency, ω, in **Fig. 1**. It should be noted that, although only one harmonic is sufficient for this case to determine accurately the amplitude and the real part of the stability factor (RSF), the prediction of imaginary part of the stability factor (ISF) requires inclusion of higher order harmonics. Therefore, first 30 harmonics are included in the analysis – in order to capture the variation of the ISF for lower excitation frequencies. For the linear structure, RSF is constant over the whole frequency range

and is equal to $c\omega_1/2$. ISF is represented as a piecewise function by a set of straight lines with zero values at the resonance frequencies excited by 1st and all higher harmonics of ω, i.e. at frequencies ω_1/m, where m is the harmonic number. Their slopes are equal to the harmonic numbers and the absolute value of ISF does not exceed the natural frequency of the system: $\omega_1=\sqrt{40}$, so for $\omega>2\omega_1$ ISF $=\pm\omega_1$

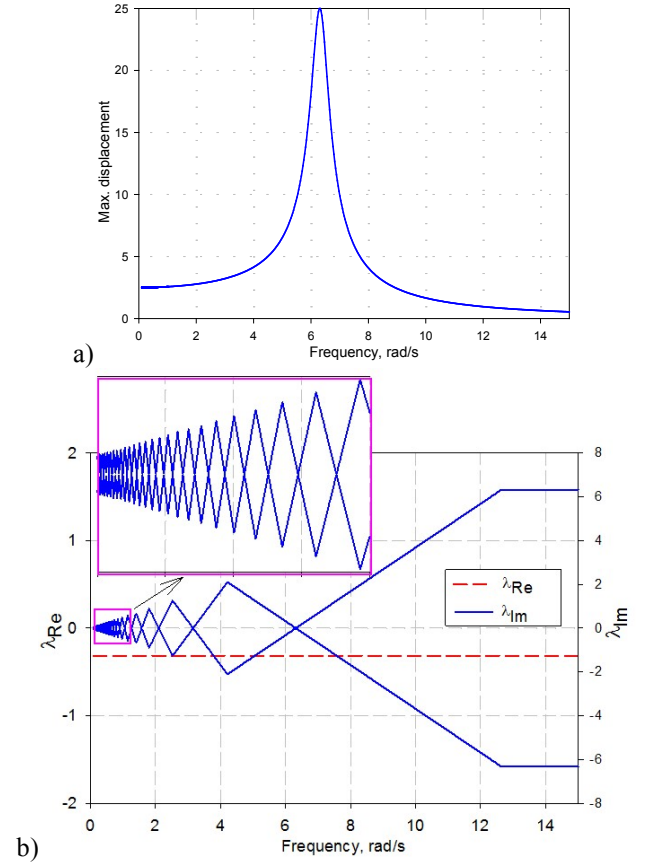

Fig. 1 Amplitude (a) and stability factors (b) of the linear oscillator

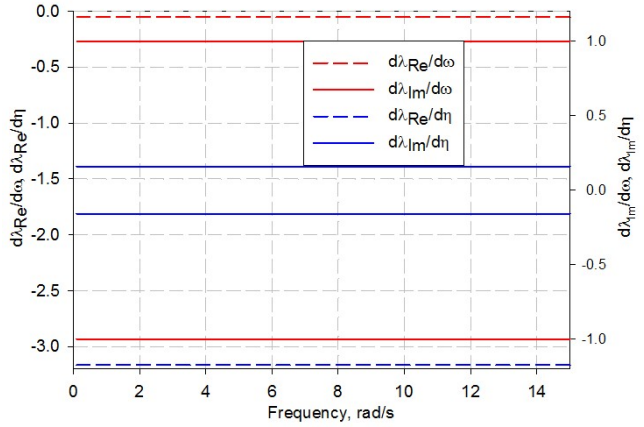

Fig. 2 Sensitivities of RSF and ISF with respect to natural frequency and modal damping variations

The sensitivity of the stability factors to modal properties of the system: the natural frequency, ω_1, and modal damping factor, η_1 are plotted in **Fig. 2**. The sensitivities are constant over the whole frequency range. As expected, the RSF is much more sensitive to the modal damping variation than to the frequency variation, the sensitivities are negative which indicates that the increase of the damping and natural frequency increases the vibration stability. ISF is more sensitive to the natural frequency variation than to the damping variation.

Cubic nonlinear spring. For the cubic spring nonlinearity the nonlinear force function is assumed: $f(x)=k_3x^3$ with $k_3=10$; The dependency of the maximum forced response on the excitation frequency is shown in **Fig. 3** where, for the plot of maximum amplitude, a blue curve indicates stable vibration regimes and a red curve corresponds to unstable vibrations. Red and blue dots on the plots of the stability factors show two stability factors. On the plot of real parts of the stability factors, λ_{Re}, the values differs only for regimes which are unstable and on the plot of imaginary parts of the stability factors, λ_{Im}, the values are here the same for the unstable regimes.

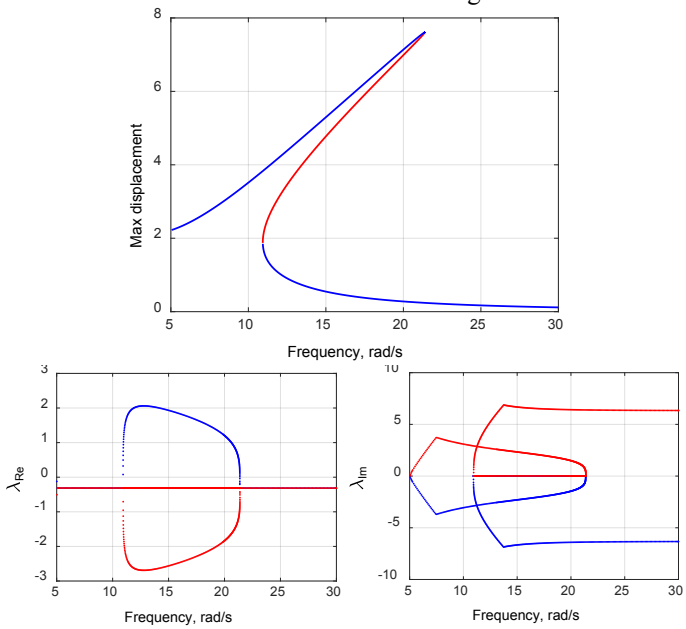

Fig. 3 The maximum displacement and the stability factors: cubic nonlinearity

The sensitivity of the λ_{Re} and λ_{Im} to the value of cubic spring stiffness, k_3, is shown in **Fig. 4** and **Fig. 5**. Moreover, in **Fig. 4** the sensitivity stability factors are compared for different numbers of harmonics kept in the multiharmonic stability analysis: (i) 3 harmonics from 0 to 2; (ii) 6 harmonics from 0 to 5 and (iii) 11 harmonics from 0 to 10. It is evident that results are practically coinciding and keeping 3 first harmonics is sufficient to achieve accurate results for the stability sensitivity. The colours used for the plotting sensitivities in **Fig. 5** correspond to the colours used for plotting the stability factors in **Fig. 3** which allow establishing the correspondence of the stability factors and

their sensitivities for two factors plotted here. The same colour scheme correspondence is used for plotting sensitivities further on in this paper. From the results obtained we can conclude that λ_{Re} is sensitive to the variation of cubic stiffness value only for unstable vibration regimes where the increase of this stiffness decreases the λ_{Re}. Variation of k_3 affect λ_{Im} over the whole frequency range analysed. The sensitivity $\partial\lambda_{Im}/\partial k_3$ grows with the decrease of excitation frequency from 10 to 5 rad/s. Both sensitivities, $\partial\lambda_{Re}/\partial k_3$ and $\partial\lambda_{Im}/\partial k_3$ has a discontinuity at two points of the solution trajectory where the vibration regime changes from stable to unstable and back

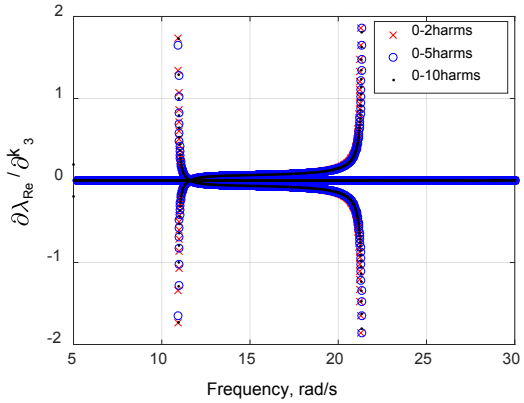

Fig. 4 Stability sensitivity $\partial\lambda_{Re}/\partial k_3$

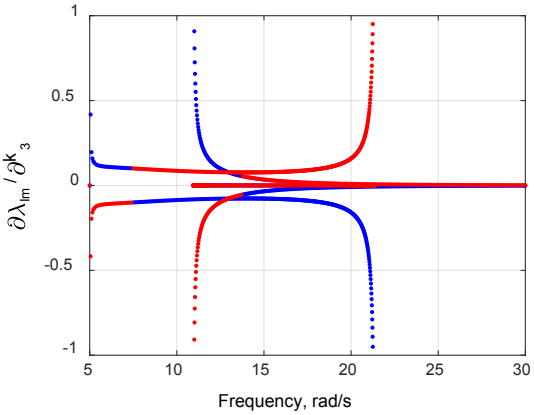

Fig. 5 Stability sensitivity $\partial\lambda_{Im}/\partial k_3$

The sensitivities of the stability factors to variation of modal properties of the linear part of the oscillator: (i) natural frequency ω_l and (ii) modal damping factor, η_l are plotted in **Fig. 6** and **Fig. 7**.

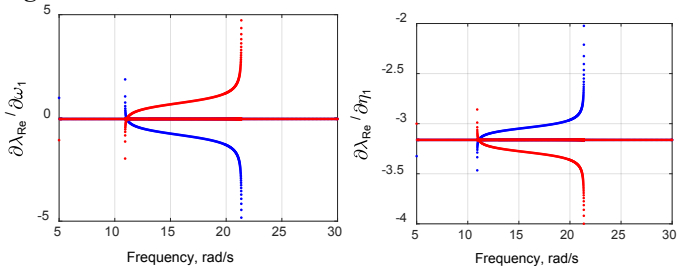

Fig. 6 Stability sensitivity $\partial\lambda_{Re}/\partial\omega_l$ and $\partial\lambda_{Re}/\partial\eta_l$

We can see that the λ_{Re} is sensitive to the variation of ω_l only for the unstable regimes and its sensitivity to η_l is constant over the whole frequency range except of the unstable regimes. Since $\partial\lambda_{Re}/\partial\eta_l$ is negative the increase of the modal damping increases the stability of the vibrations. The sensitivity $\partial\lambda_{Re}/\partial\omega_l$ is negative for the stability factor with positive real part, therefore the increase of the natural frequency can decrease λ_{Re} and, hence, the speed of the amplitude growth of the perturbed motion when it leaves the unstable vibration regime.

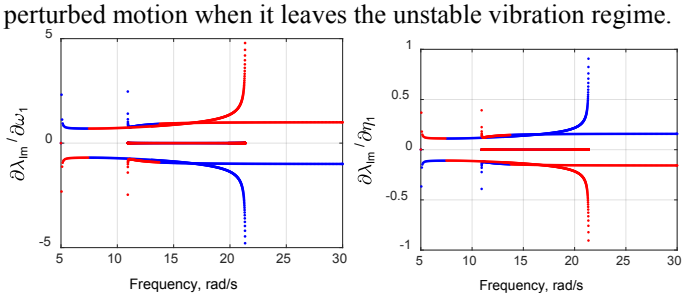

Fig. 7 Stability sensitivities $\partial\lambda_{Im}/\partial\omega_l$ and $\partial\lambda_{Im}/\partial\eta_l$

Gap nonlinearity. For the gap nonlinearity the nonlinear force function is assumed to be $f(x)=k_{gap}x$ for $x>=g$ and $f(x)=0$ for $x<g$ where $k_{gap}=400$ and $g=10$. The forced response amplitudes are shown in **Fig. 8** together with the real and imaginary parts of the stability factors. The sensitivity of λ_{Re} with respect to the additional stiffness, k_{gap}, which come to effect when the gap is closed and with respect to gap value, g, are shown in **Fig. 9** and **Fig. 10**.

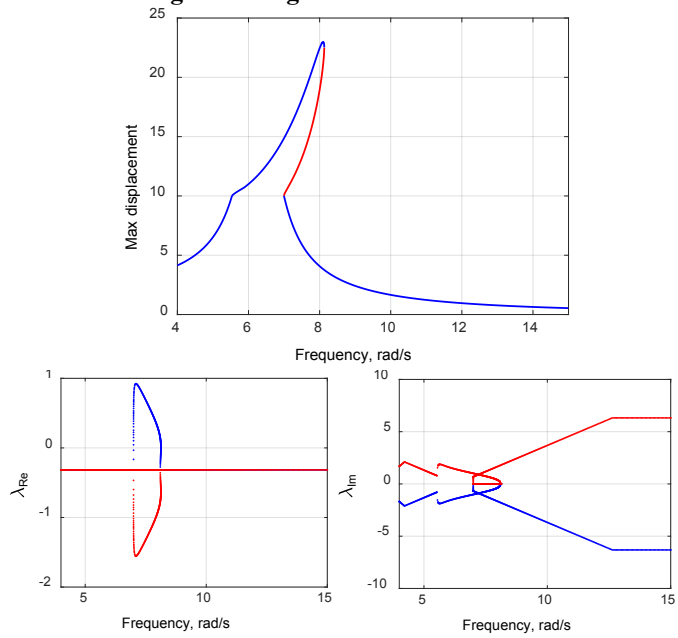

Fig. 8 The maximum displacement and stability factors: gap nonlinearity

One can see that the sensitivities with respect to both gap contact interface parameters are zero for stable vibration regimes and rather sensitive to the gap stiffness and to gap value for

unstable vibrations. The sensitivity of λ_{Re} to gap value is close to constant for unstable regimes and grows to infinity within vicinity of the points where the system changes its stable/unstable stability property.

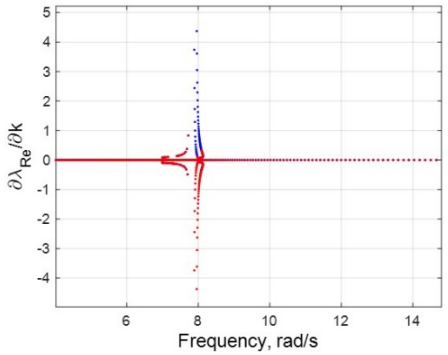

Fig. 9 Stability sensitivity $\partial\lambda_{\mathrm{Re}}/\partial k_{gap}$

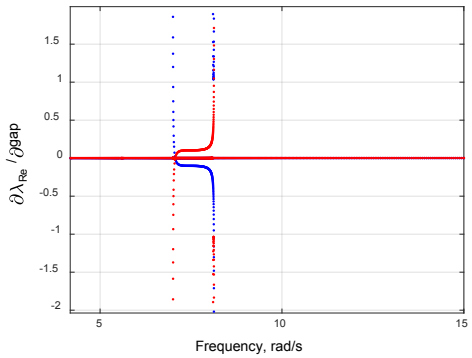

Fig. 10 Stability sensitivity $\partial\lambda_{\mathrm{Re}}/\partial gap$

Friction nonlinearity. For the friction nonlinearity the model developed in Ref.[4] is used with the friction coefficient, $\mu = 0.3$; the tangential contact stiffness, $k_t = 100$ and the normal force, $N_0 = 800$. The calculated forced response is displayed in and the stability factors are shown in **Fig. 11**.

The sensitivity of the real parts of the stability factors, λ_{Re}, to parameters of friction contact interface μ and k_t area shown in **Fig. 12** and **Fig. 13**. The sensitivity with respect to the normal pressure, N_0, applied at the friction contact interface is not plotted here since for the case considered here, when the normal pressure is not varied in time, the friction limiting force is calculated as a product μN_0 and the sensitivity $\partial\lambda_{\mathrm{Re}}/\partial N_0$ differs from $\partial\lambda_{\mathrm{Re}}/\partial\mu$ only by a multiplier, i.e. $\mu\partial\lambda_{\mathrm{Re}}/\partial\mu = N_0\partial\lambda_{\mathrm{Re}}/\partial N_0$. The results of validation of the developed sensitivity analysis method is also displayed in **Fig. 12**, where the sensitivity coefficients based on the developed method where the sensitivity are based on exact analytically derived expressions are compared with the results based on finite difference approximation of the stability factor sensitivities:

$$\partial\lambda/\partial\mu \approx \left[\lambda(\mu+\Delta\mu)-\lambda(\mu)\right]/\Delta\mu \qquad (42)$$

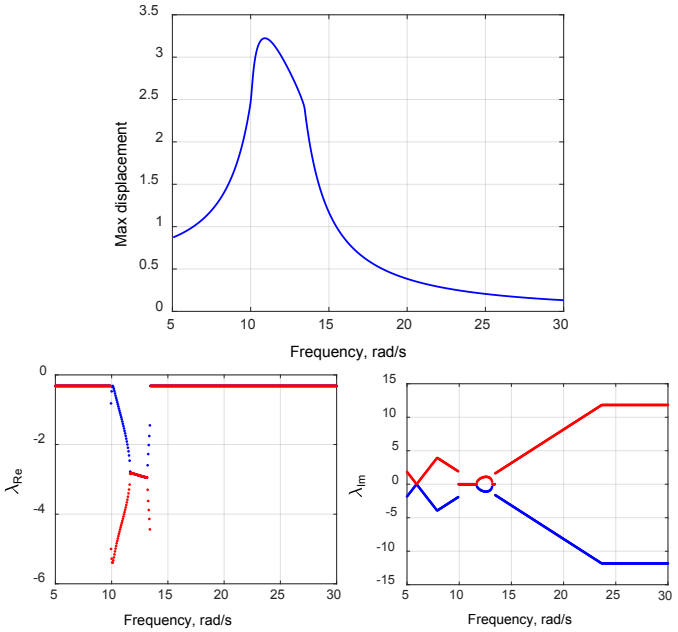

Fig. 11 Dependency of the maximum displacement and stability factors on excitation frequency: friction contact

To obtain the finite difference sensitivity approximations the stability analysis is performed two times: (i) first time with the nominal values of the contact interface parameters and (ii) second time with the small variation of the contact interface parameter. For the case considered here the second analysis is performed with $\mu = 0.30001$. Similar validations have been performed for all types of the nonlinear elements and their contact parameters considered in this paper. One can see excellent correspondence between the finite difference approximations and the values provided by the developed method. It should be noted that the finite difference sensitivity analysis is not also much more time consuming and less accurate than those provided by the method developed, but also in many cases such analysis cannot be performed, e.g. when the nonlinear solution curves are multivalued and more complex than for the case of the oscillator with a single friction damper.

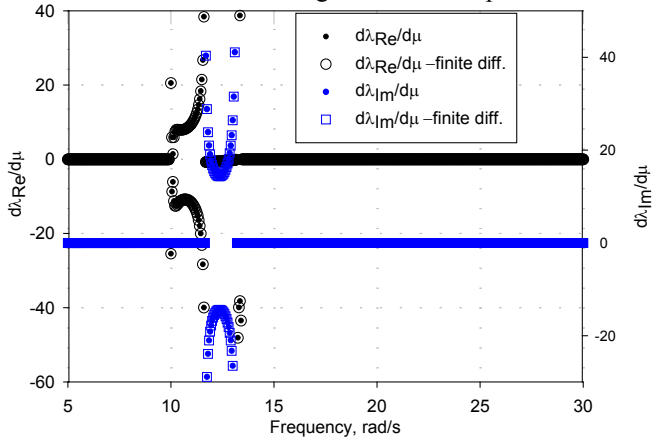

Fig. 12 Stability sensitivity $\partial\lambda_{\mathrm{Re}}/\partial\mu$

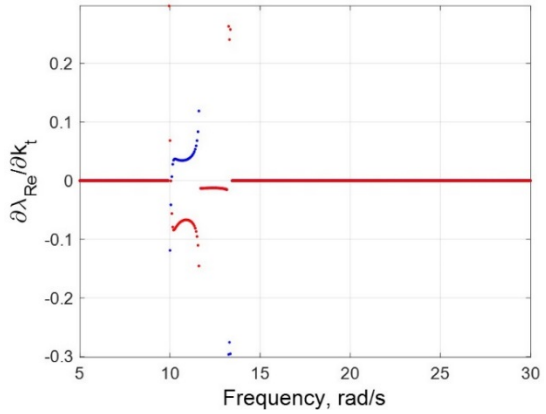

Fig. 13 Stability sensitivity $\partial\lambda_{\mathrm{Re}}/\partial k_t$

From **Fig. 12** and **Fig. 13** we can notice that the sensitivities with respect to parameters of friction contact interface $\partial\lambda_{\mathrm{Re}}/\partial\mu$ and $\partial\lambda_{\mathrm{Re}}/\partial k_t$ differs from zero only for frequency ranges where slip occurs and the friction damper starts to operate. Since the sensitivity can take positive values for one of the two stability factors the increase of the friction coefficient or the contact stiffness can decrease the rate with which the perturbed motion decays and returns to the stable vibration regime – in other words it might make the vibration less stable, although not changing the stability property when the variation is small.

A cantilever beam

Another model analysed is a cantilever beam with sides 1000×200×100mm and with the following material properties: elasticity modulus E=10^{5}N/mm^2; density ρ=4.43*10^{-9}Mg/mm^3. 8 finite element beam model is used for the stability sensitivity analysis and the total number of DOFs in the model is 32. The case of viscous damping is considered – to be able to compare the results with the classical time-domain integration approach for the calculation of the Floquet exponents. The modal damping factors of the beam are 0.02 for all mode shapes. The cubic nonlinear spring is applied at the free end of the cantilever beam with stiffness coefficient $k_3 = 10^6$ N/mm^3. The excitation force is applied also at the free end of the beam and the amplitude of the excitation force is 100N. First 6 harmonics are included in the multiharmonic stability analysis: from 0 to 5. The forced response calculated at the beam end is plotted in **Fig. 14**.

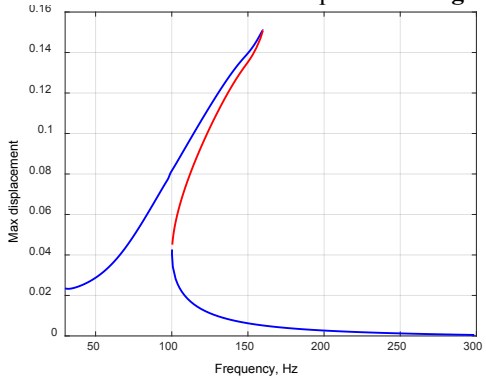

Fig. 14 Amplitudes of a beam with cubic nonlinearity

The real and imaginary parts of two stability factors which have largest real part values and which define the stability of the vibrations are shown in **Fig. 15**. Here, stability factors calculated by using the reduced stability model are shown and the results are compared when different number of mode shapes are included in the stability reduced basis, namely: 1, 2, 4, 8 and 16. Moreover, the Floquet exponents are calculated by a classical procedure: by integration of the time domain stability equation with full 8 finite element beam model to obtain the monodromy matrix and to calculate its eigenvalues. So in this figure the analysis of accuracy of the proposed multiharmonic sensitivity analysis method is verified by comparison with the results of Floquet stability analysis and also effect of the number of modes kept in the reduced model is assessed. One can see that: (i) when only 1 mode is used in the reduced basis the results differ significantly from the others reduced models, (ii) using 2 modes provide acceptable accuracy of the stability factors and (iii) starting form 4 modes in the reduced basis the results become undistinguishable and coinciding with the time-domain Floquet analysis.

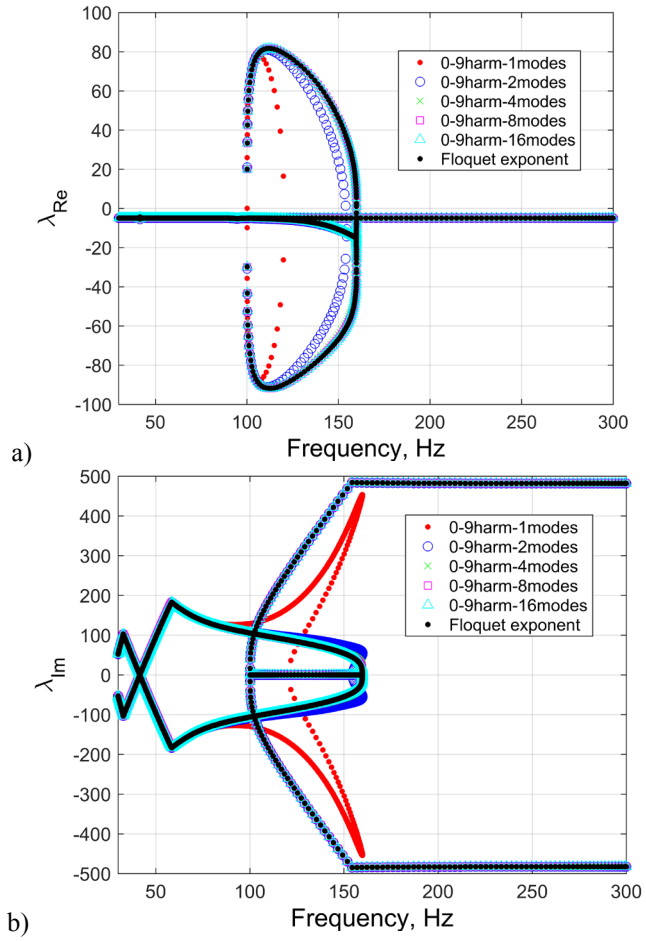

Fig. 15 Selected stability factors for the block with cubic nonlinearity: effect of the number of mode shapes

The stability factor sensitivity $\partial\lambda_{\mathrm{Re}}/\partial k_3$ is displayed in **Fig. 16**. Here, the effect of using in the reduced stability model

different number of mode shapes is explored on the accuracy of calculation of the stability sensitivities.

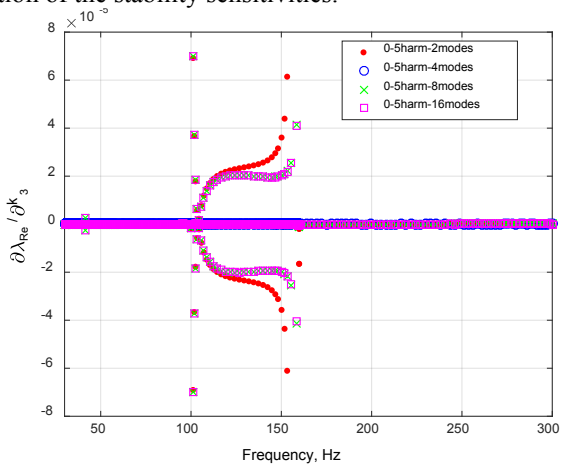

Fig. 16 Stability sensitivity $\partial\lambda_{\mathrm{Re}}/\partial k_3$

One can see that, similar to the analysis of the stability factors, when we study the stability sensitivity we observe that starting from 4 mode shapes the values of sensitivities are practically coinciding and in the practical analysis of this beam we can use just 4 modes in the reduced stability model. The sensitivity, $\partial\lambda_{\mathrm{Re}}/\partial k_3$, is close to zero everywhere except of the unstable regimes of vibrations. Since $\partial\lambda_{\mathrm{Re}}/\partial k_3$ corresponding to stability factor with positive λ_{Re} is negative, we can conclude that increase of the cubic stiffness coefficient can reduce the severity of the instability in the system.

The sensitivity of the stability factors to variation of 1st natural frequency and modal damping factor is shown for this beam in **Fig. 17** and **Fig. 18**. From these plots we can see that $\partial\lambda_{\mathrm{Re}}/\partial\omega_1$ differs significantly from zero only for unstable vibration regimes where the sensitivity of the stability factor with positive real part is negative. The sensitivity $\partial\lambda_{\mathrm{Re}}/\partial\eta_1$ is negative and frequency independent for stable regimes and for unstable regimes it still negative although it increases its values

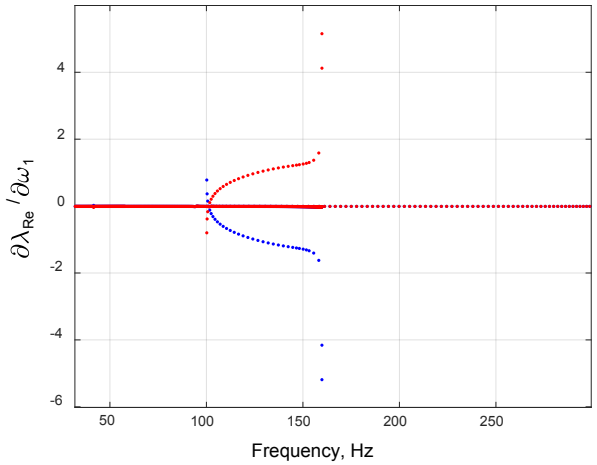

Fig. 17 Stability sensitivity $\partial\lambda_{\mathrm{Re}}/\partial\omega_1$

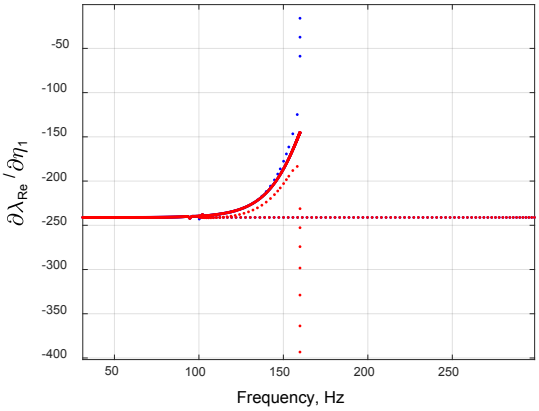

Fig. 18 Stability sensitivity $\partial\lambda_{\mathrm{Re}}/\partial\eta_1$

A turbine blade

Another example considered is a cooled turbine blade with the finite element model shown in **Fig. 19** and which comprises 160,000 DOFs. The blade is fixed at the blade root contact patches (marked in red in the figure) and the excitation forces are distributed over blade airfoil. The damping is frequency-independent with all modal damping factors equal to 0.02. 22 cubic nonlinear spring elements are distributed over a contact patch of the blade shroud (marked in yellow in the figure). In the multiharmonic forced response analysis 6 harmonics are used: from 0 to 5 and for the reduced stability model 12 blade modes are used.

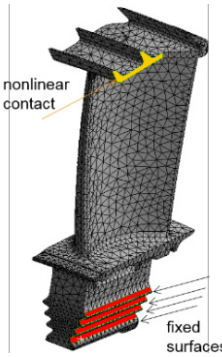

Fig. 19. A cooled turbine blade: a finite element model

The calculated forced response is plotted in **Fig. 20** and the stability factors are plotted in **Fig. 21**.

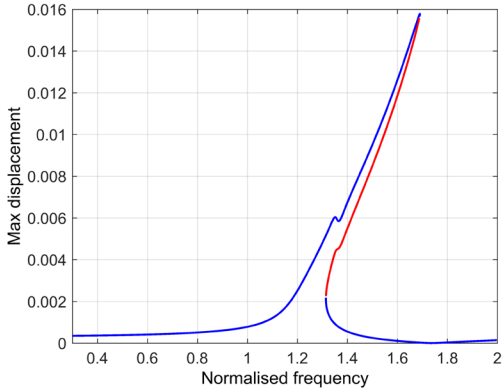

Fig. 20 Amplitudes of the turbine blade nonlinear response

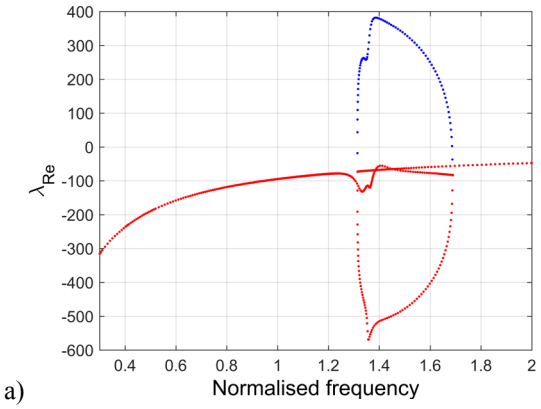

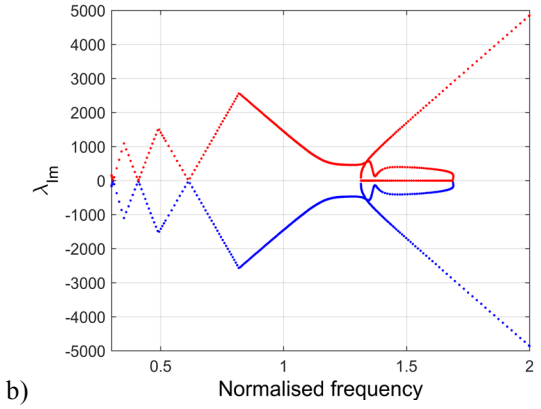

Fig. 21 Stability factors of the turbine blade

The sensitivities of the stability factors to the cubic stiffness coefficient value are shown in **Fig. 22** and **Fig. 23**. We can see that the real part of the stability factor is dependent on the variation of the cubic stiffness coefficient only for unstable vibration regimes, while the imaginary part of the stability factor is sensitive to this stiffness over a wide frequency range. The variation of the stability sensitivity, $\partial\lambda_{Im}/\partial k_3$, with variation of the excitation frequency differs significantly from the case of 1DOF oscillator considered earlier: this is due to the multiple contacting nodes of the FE model and also due to more complex vibration mode of vibration of the turbine blade.

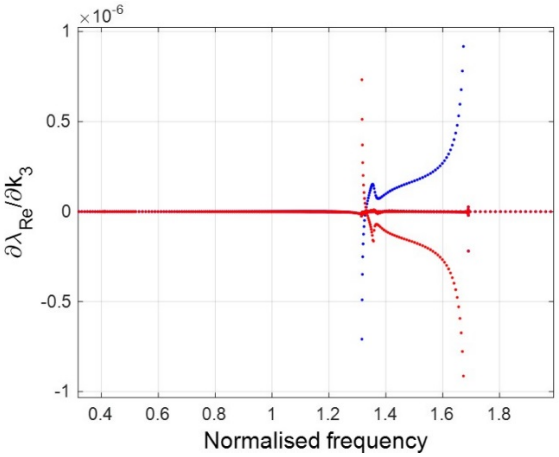

Fig. 22 Stability sensitivity $\partial\lambda_{Re}/\partial k_3$

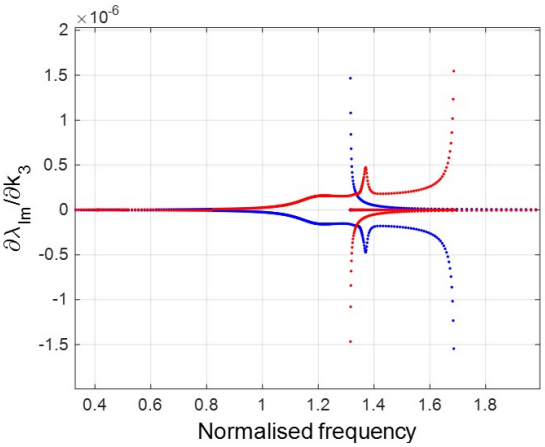

Fig. 23 Stability sensitivity $\partial\lambda_{Im}/\partial k_3$

The sensitivities of the real part of the stability factors to natural frequencies and modal damping values are shown in **Fig. 24** and **Fig. 25** for first 3 vibration modes. One can see that λ_{Re} is the most sensitive to the modal characteristics of 1st vibration mode. The modal damping values of 2nd and 3rd modes affect λ_{Re} when the vibrations are unstable, while λ_{Re} is highly sensitive to the modal damping of first mode over the whole frequency range analysed.

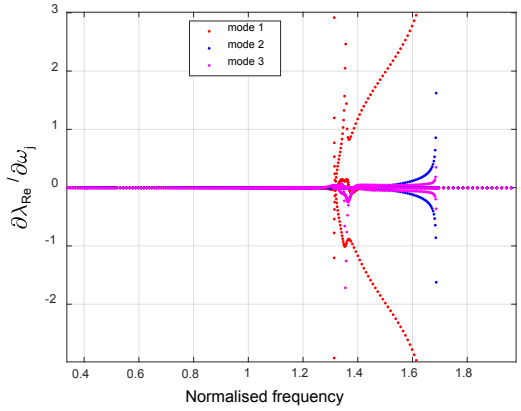

Fig. 24 Stability sensitivity $\partial\lambda_{Re}/\partial\omega_j$ for different modes

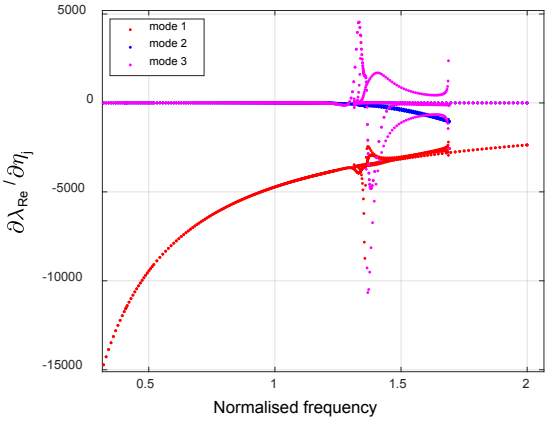

Fig. 25 Stability sensitivity $\partial\lambda_{Re}/\partial\eta_j$ for different modes

CONCLUSIONS

A method has been developed for the stability sensitivity analysis of nonlinear vibrations using large models of gas-turbine and other structures with nonlinear contact interfaces. This is a first formulation, development and implementation of this problem known in the literature, to the best of the author's knowledge.

The method allows an efficient frequency-domain analysis of analytically derived and, therefore, highly accurate sensitivities of the stability factors to variation of design parameters of a structure. The multiharmonic representations of nonlinear displacements and forces are used which provide high accuracy for the periodic vibration regime calculation. The formulations have been proposed for cases when the design parameters of an assembled structure with joints include: (i) dynamic properties of linear components of the structure, e.g. its natural frequencies and modal damping factors, geometry, material properties, etc. and (ii) parameters of the nonlinear contact interfaces, such as friction coefficient, tangential and normal stiffness coefficients of the rough surfaces of a contact interface; clearance and interference values, contact stiffness of cubic nonlinearity and others. Moreover, the cases of full stability models and reduced stability models are considered.

The efficiency of the method and new approaches are demonstrated on relatively simple systems and on a large-scale model of a cooled turbine blade. Effects of the number of harmonics and the number of mode shapes used in the reduced stability modelling have been assessed. The examples of studies of sensitivity stability with respect to modal properties of the models and parameters of cubic nonlinear springs, gaps and friction nonlinearities are provided.

REFERENCES

[1] C. Pierre, A. A. Ferri and E. H. Dowell, (1985) "Multi-harmonic analysis of dry friction damped systems using an incremental harmonic balance method", *J. Appl. Mech. ASME*, 52, pp.958-964 (1985).

[2] Cardona, A., Coune, T., Lerusse, A., and Geradin, M., (1994) "A multiharmonic method for nonlinear vibration analysis", *Int. J. for Num. Meth. in Eng.,* Vol. 37, No. 9, pp. 1593-1608

[3] Chen, J., Menq, C., (2001), "Prediction of periodic response of blades having 3D nonlinear shroud constraints," *J. of Eng. for Gas Turbines and Power*, Vol. 123, pp. 901-909.

[4] Petrov, E.P., Ewins, D.J., 2003, "Analytical formulation of friction interface elements for analysis of nonlinear multi-harmonic vibrations of bladed discs", *ASME J. of Turbomachinery*, Vol.125, pp.364-371

[5] Zucca, S., C.M. Firrone, and M.M. Gola, (2012). Numerical assessment of friction damping at turbine blade root joints by simultaneous calculation of the static and dynamic contact loads. *Nonlinear Dynamics*, 67(3): p. 1943-1955.

[6] Laborenz, J., M. Krack, et al. (2012). "Eddy Current Damper for Turbine Blading: Electromagnetic Finite Element Analysis and Measurement Results." *J. of Eng. for Gas Turbines and Power*, 134(4).

[7] Batailly, A., M. Legrand, et al. (2012). "Numerical-experimental comparison in the simulation of rotor/stator interaction through blade-tip/abradable coating contact." *J. of Eng. for Gas Turbines and Power*, 134(8).

[8] Petrov, E., (2015) "Analysis of bifurcations in multiharmonic analysis of nonlinear forced vibrations of gas-turbine engine structures with friction and gaps", Proc. of ASME Turbo Expo 2015, June 15 – 19, 2015, Montréal, Canada, GT2015-43670, 12 pp.

[9] Floquet, G. (1883). "Sur les équations différentielles linéaires à coefficients périodiques", Annales scientifiques de l'É.N.S. 2e série, tome 12, p. 47-88.

[10] Peletan, L., et al. (2013). "A comparison of stability computational methods for periodic solution of nonlinear problems with application to rotordynamics." Nonlinear Dynamics 72(3): 671-682

[11] Lewandowski, R. (1997). "Computational formulation for periodic vibration of geometrically nonlinear structures .1. Theoretical background." Int. J. of Solids and Structures 34(15): 1925-1947

[12] Von Groll, G. and Ewins, D.J. (2001) "The harmonic balance method with arc-length continuation in rotor/stator contact problems", *J. of Sound and Vibration*, v 241, n 2, p 223-233

[13] Villa, C., J.-J. Sinou, and F. Thouverez (2008). "Stability and vibration analysis of a complex flexible rotor bearing system." Communications in Nonlinear Science and Numerical Simulation 13(4): 804-821.

[14] Lazarus, A. and O. Thomas (2010). "A harmonic-based method for computing the stability of periodic solutions of dynamical systems." Comptes Rendus Mecanique 338(9), pp. 510-517.

[15] T. Detroux, L. Renson, L. Masset, G. Kerschen (2015). The harmonic balance method for bifurcation analysis of large-scale nonlinear mechanical systems", Comput. Methods Appl. Mech. Engrg. 296 (2015) 18–38

[16] E. Petrov, "Stability analysis of multiharmonic nonlinear vibrations for large models of gas-turbine engine structures with friction and gaps", Proc. of ASME Turbo Expo 2016, June 13 – 17, Seoul, South Korea, GT2016-57959

[17] Petrov, E.P, (2009) "Analysis of sensitivity and robustness of forced response for nonlinear dynamic structures", *Mechanical Systems and Signal Processing*, Vol. 23, pp. 68– 86

[18] Petrov,E.P., (2011) "A high-accuracy model reduction for analysis of nonlinear vibrations in structures with contact interfaces", *Trans. ASME J. Eng. for Gas Turbines and Power*, Vol. 133, March, 2011.

[19] Petrov, E.P., "Sensitivity Analysis of Nonlinear Forced Response for Bladed Discs with Friction Contact Interfaces", Proc. of ASME Turbo Expo 2005, June 6–9, 2005, Reno-Tahoe, USA, GT2005-68935

[20] Petrov, E.P., (2004) "Method for direct parametric analysis of nonlinear forced response of bladed discs with friction contact interfaces", Trans. ASME: J. of Turbomachinery, Vol.126, October, pp.654-662